

DecoKAN: Interpretable Decomposition for Forecasting Cryptocurrency Market Dynamics

Yuan Gao, Zhenguo Dong, Xuelong Wang, Zhiqiang Wang, Yong Zhang, *Member, IEEE*, and Shaofan Wang

Abstract—Accurate and interpretable forecasting of multivariate time series is crucial for understanding the complex dynamics of cryptocurrency markets in digital asset systems. Advanced deep learning methodologies, particularly Transformer-based and MLP-based architectures, have achieved competitive predictive performance in cryptocurrency forecasting tasks. However, cryptocurrency data is inherently composed of long-term socio-economic trends and local high-frequency speculative oscillations. Existing deep learning-based ‘black-box’ models fail to effectively decouple these composite dynamics or provide the interpretability needed for trustworthy financial decision-making. To overcome these limitations, we propose DecoKAN, an interpretable forecasting framework that integrates multi-level Discrete Wavelet Transform (DWT) for decoupling and hierarchical signal decomposition with Kolmogorov–Arnold Network (KAN) mixers for transparent and interpretable nonlinear modeling. The DWT component decomposes complex cryptocurrency time series into distinct frequency components, enabling frequency-specific analysis, while KAN mixers provide intrinsically interpretable spline-based mappings within each decomposed subseries. Furthermore, interpretability is enhanced through a symbolic analysis pipeline involving sparsification, pruning, and symbolization, which produces concise analytical expressions offering symbolic representations of the learned patterns. Extensive experiments demonstrate that DecoKAN achieves the lowest average Mean Squared Error on all tested real-world cryptocurrency datasets (BTC, ETH, XMR), consistently outperforming a comprehensive suite of competitive state-of-the-art baselines. These results validate DecoKAN’s potential to bridge the gap between predictive accuracy and model transparency, advancing trustworthy decision support within complex cryptocurrency markets.

Index Terms—Cryptocurrency, Time Series Forecasting, Kolmogorov–Arnold Networks, Wavelet Transform.

I. INTRODUCTION

CRYPTOCURRENCY systems generate massive volumes of time series data by continuously recording observations and events over extended periods. Accurate forecasting of such data has become essential for optimizing investment strategies, managing market risks, and maintaining economic stability. For example, forecasting trading volume enables better liquidity management to cope with market panic, while predicting price volatility contributes to the design of more resilient decentralized finance (DeFi) protocols [1], [2]. The

This work was supported by the Beijing Municipal Natural Science Foundation (No. L251067), the Fundamental Research Funds for the Central Universities (No. 3282024058, 3282024052), and the China Postdoctoral Science Foundation (No. 2019M650608). (Corresponding author: Zhiqiang Wang.)

Yuan Gao, Zhenguo Dong, Xuelong Wang, and Zhiqiang Wang are with the Beijing Electronic Science and Technology Institute, Beijing 100070, China. Yong Zhang and Shaofan Wang are with the Beijing University of Technology, Beijing 100124, China. (E-mail: gy@besti.edu.cn; dongzgxx@163.com; 20243806@mail.besti.edu.cn; wangzq@besti.edu.cn; zhangyong2010@bjut.edu.cn; wangshaofan@bjut.edu.cn).

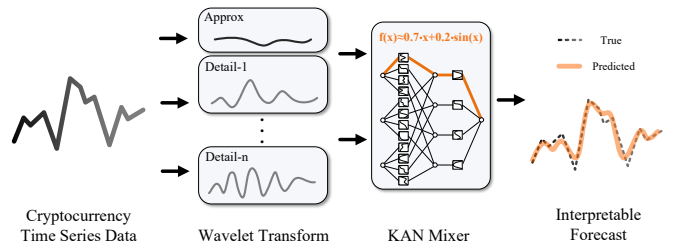


Fig. 1. Conceptual overview of the DecoKAN framework for interpretable time series forecasting.

complex nature of cryptocurrency markets, effectively functioning as large-scale computational social systems driven by heterogeneous agent interactions [3], characterized by interdependencies among variables and dynamics across multiple temporal scales, necessitates robust and trustworthy forecasting methodologies.

Early efforts in time series forecasting primarily relied on traditional statistical methods. Models from the Autoregressive Integrated Moving Average (ARIMA) family, including seasonal variants such as SARIMA and extensions incorporating exogenous variables like ARIMAX, established a strong statistical foundation for time series forecasting [4]. These statistical approaches offered simplicity and, importantly, high interpretability through transparent mathematical formulations that explicitly model trend, seasonality, and linear dependencies. In parallel, conventional machine learning techniques such as Hidden Markov Models (HMMs) were also explored, providing a probabilistic framework to better capture dynamic non-linear behaviors in financial time series [5]. However, both traditional statistical and early machine learning models often struggled to represent the highly non-linear patterns, abrupt shifts, long-range dependencies, and intricate cross-variable relationships typical of large-scale financial time series, particularly within the volatile and dynamic digital financial market [6].

Deep learning methods have subsequently emerged as powerful tools for addressing these challenges, leveraging their strong nonlinear modeling capabilities. Early approaches employed Recurrent Neural Networks (RNNs), such as Long Short-Term Memory (LSTM) networks, and Convolutional Neural Networks (CNNs) adapted for sequential data [7]. Later, Transformer-based architectures [8] became dominant due to their ability to model long-term dependencies, with models like Informer [9], Autoformer [10], and FEDformer [11] achieving notable success, while Non-stationary Transformers [12] aimed to mitigate distributional shifts. In the

specific context of cryptocurrency trading, researchers have further tailored these architectures to address domain-specific challenges. For instance, recent works have enhanced Transformer models with market sentiment indices with advanced market sentiment analysis [13] to improve prediction accuracy, and integrated diverse data sources—combining financial, on-chain, and social media metrics—to capture complex market dynamics [14]. More recent architectures, including PatchTST [15] and iTransformer [16], further optimized Transformer efficiency and locality. In parallel, motivated by studies questioning the necessity of complex attention mechanisms for all forecasting tasks, several simpler yet competitive MLP-based architectures have been proposed, including DLinear [17], TimeMixer [18], TSMixer [19] and WPMixer [20]. These models often employ decomposition techniques, such as moving averages (TimeMixer) or wavelet transforms (WPMixer), to improve predictive robustness. Other CNN-based models such as TimesNet [21] and TimeXer [22] extend the MLP-Mixer paradigm [23], further enriching the design space. Collectively, these developments have substantially advanced the state-of-the-art in forecasting accuracy. However, directly applying these Transformer-based and MLP-based architectures to cryptocurrency price prediction remains problematic. These general-purpose models often struggle to adapt to the idiosyncrasies of cryptocurrency data, such as its extreme volatility, regime-switching non-stationarity, and the intricate mixture of long-term adoption trends with high-frequency speculative noise. Consequently, applying these sophisticated models in this context faces two fundamental challenges.

Challenge 1: Decoupling and Modeling Composite Signals. Cryptocurrency time series display complex temporal patterns that combine long-term structural trends with short-term volatility and noise. Explicitly decomposing and modeling these distinct components separately, rather than as a mixed signal, remains a challenge for most conventional forecasting architectures.

Challenge 2: Lack of interpretability. Although modern deep learning models achieve strong predictive accuracy, they often operate as opaque black boxes, offering little insight into their internal reasoning. This lack of transparency undermines trust and hinders adoption, particularly in the high-stakes financial contexts of DeFi and digital assets.

A review of existing approaches reveals both substantial progress and persistent limitations. Traditional statistical methods are interpretable but fail to capture the nonlinear complexity of market dynamics. Advanced deep learning models deliver higher accuracy, and certain architectures, such as WPMixer [20], employ decomposition strategies to decouple the composite signals. Nevertheless, while these decomposition-based frameworks separate the components, they still rely on opaque black boxes for modeling. For signal decomposition, the Discrete Wavelet Transform (DWT) provides an established and effective method of separating signals into distinct components. At the same time, the persistent black-box nature of high-performance models continues to impede transparency and auditability, which are essential for trust and risk management in financial decision-making systems. Recently, the Kolmogorov-Arnold Network (KAN) paradigm

has emerged as a promising direction, offering intrinsic interpretability through learnable spline activations and explicit symbolic representations [24], [25]. The potential of applying the combination of KAN’s symbolic transparency and DWT’s proven capability in decomposing multivariate time series data to cryptocurrency market data remains unexplored.

To bridge this gap, we propose DecoKAN (conceptually illustrated in Fig. 1), a novel interpretable forecasting framework that synergistically combines the hierarchical decomposition capabilities of DWT with the transparent, non-linear modeling power of KANs. Fig. 1 illustrates the core concept: cryptocurrency time series data is decomposed by wavelet transform, processed by a KAN-based mixer, and reconstructed into an interpretable forecast. This design enables accurate forecasting of complex market dynamics while maintaining transparent internal reasoning and scrutable logic. Our contributions can be summarized as follows:

(1) In this paper, a novel framework named DecoKAN is proposed, which applies multi-level Discrete Wavelet Transform (DWT) to decompose composite financial time series into distinct approximation and detail components. Each component is then processed independently within dedicated Resolution Branches, thereby isolating the processing of distinct frequency bands and allowing for specialized pattern learning.

(2) A Kolmogorov–Arnold Network (KAN)-based mixer is introduced to address the opacity of conventional architectures. By replacing standard MLP layers with learnable spline activation functions, this mixer provides intrinsic interpretability and enables precise, transparent modeling of the relationships specific to each decoupled component, preserving the unique information captured by the wavelet decomposition.

(3) Extensive experiments demonstrate that DecoKAN achieves state-of-the-art long-term forecasting performance on benchmark and cryptocurrency datasets while offering robust interpretability through symbolic explanations.

II. RELATED WORK

A. Deep Learning Models for Time Series Forecasting

Deep learning methods have become central to time series forecasting as data availability and computational capacity increase [26]. Transformer architectures, capable of modeling long-range dependencies, remain widely used. Representative models include Informer [9], Autoformer [10], FEDformer [11], and Crossformer [27], while recent variants such as PatchTST [15] and iTransformer [16] enhance local semantic capture with improved efficiency. Some approaches also explore probabilistic forecasting [28] and generative pre-training for time series [29]. Despite these advances, their internal reasoning remains difficult to interpret [8], [30], [31]. More recent work explores MLP-based architectures as lightweight yet competitive alternatives. Zeng et al. [17] showed that simple linear models like DLinear can rival Transformer performance on standard benchmarks. Building on this insight, methods such as TimeMixer and WPMixer integrate decomposition mechanisms to separate trend and seasonal components or to perform multi-level wavelet analysis [18], [20]. Frequency-domain approaches [32], [33] and long-term forecasting methods [34] further enhance modeling capabilities. Other variants,

including TimeXer and TimesNet, adapt MLP-Mixer and 2D-kernel designs for temporal data [19], [21], [23]. Additionally, graph-based approaches like TimeFilter [35] employ spatial-temporal graph filtration to adaptively model dependencies while filtering out irrelevant correlations.

Recent advances in deep learning have significantly improved time series forecasting performance, while decomposition-based approaches such as wavelet analysis have demonstrated strong potential for modeling and decoupling composite signals. Yet, even models employing such decomposition techniques often remain opaque, limiting their interpretability and undermining user trust in their predictions.

B. Cryptocurrency Market Time Series Forecasting

Cryptocurrency market data are characterized by volatility, non-stationarity, and the complex composite nature of long-term trends and high-frequency oscillations, all of which complicate accurate forecasting. Earlier studies relied on statistical models such as ARIMA and VAR or on classical machine learning methods including SVMs and Random Forests [4]. While interpretable, these approaches fail to capture nonlinear dynamics and sudden structural shifts typical of crypto markets. Deep learning models, from LSTMs to Transformers and recent adaptive distillation frameworks, have since been adopted for cryptocurrency forecasting [36], [37]. Hybrid architectures combining LSTM with Transformers have also emerged to leverage strengths of both approaches. However, they still struggle with the coexistence of slow, long-term trends and rapid, high-frequency fluctuations. Although wavelet decomposition effectively decouples signal components in general time series analysis, its use in digital asset analysis remains limited [38]–[40]. Furthermore, while recent studies have explored hybrid approaches combining machine learning with Large Language Models (LLMs) to balance performance and interpretability, existing methods often sacrifice decoupling capability for post-hoc explanations rather than achieving intrinsic transparency [41], [42].

Consequently, a critical research gap persists in these high-stakes financial domains: the lack of a unified methodology that can simultaneously disentangle composite socio-economic signals for high accuracy and provide the intrinsic, auditable interpretability required for trustworthy decision-making in complex social systems.

C. Interpretable Deep Learning and Kolmogorov-Arnold Networks (KANs)

Efforts to make AI systems more transparent have driven research on interpretable deep learning [43]. Two major approaches dominate the field: post-hoc explanation tools such as LIME [44] and SHAP [45], which approximate reasoning after training, and intrinsically interpretable architectures designed for transparency from the outset [46], [47]. Among these, Kolmogorov–Arnold Networks (KANs) represent a promising development [24], [25]. Instead of fixed activation functions, KANs employ learnable spline functions along their connections, enabling both strong approximation guarantees and

symbolic representation. Interpretability in KANs is achieved through a structured process of sparsification, pruning, and symbolization that converts trained models into explicit mathematical expressions. This approach unites theoretical expressiveness with explicit transparency, forming a novel path toward explainable AI. KANs have shown promise across diverse domains, including recommendation systems [48], medical image analysis [49], and various time series applications [50]. However, their application to complex, composite, and non-stationary time series, such as those in volatile financial markets, is still at an early stage [51], [52]. While concurrent work, such as Wav-KAN [53], modifies the KAN architecture itself by incorporating wavelet functions as activations, and other recent studies explore KAN for time series classification [54] and domain-specific forecasting tasks [55], [56], the effective combination of standard KANs’ symbolic transparency with hierarchical signal decomposition via DWT, specifically tailored for cryptocurrency’s distinctive temporal dynamics, remains largely unaddressed.

In essence, KANs bridge numerical learning and symbolic understanding. Their potential for interpretable forecasting is evident, yet their capacity to manage composite nature of market data has not been fully examined.

III. PROPOSED METHOD

Let $\mathcal{X} = \{x_t\}_{t=1}^N$ represent the historical multivariate time series data from a cryptocurrency market, where N denotes the total length of the series. Each $x_t \in \mathbb{R}^{1 \times C}$ constitutes an observation vector at time t , encompassing C variates (e.g., transaction flows, market volatility, or token prices). Given the historical sequence over a look-back window of length L , denoted as $X_L = \{x_{t-L+1}, \dots, x_t\}$, our objective is to learn a mapping F to forecast the future sequence $X_T = \{x_{t+1}, \dots, x_{t+T}\}$ over a prediction horizon of length T . This forecast, representing the anticipated evolution of these key market indicators, is crucial for applications ranging from financial decision-making to quantitative investment analysis. The forecasting task can be formally expressed as:

$$X_T = F(X_L) \quad (1)$$

where X_T is the predicted future sequence.

A. Model Architecture

To effectively model the disparate dynamics inherent in cryptocurrency markets, the architecture of our proposed model, DecoKAN, follows the principled decompose-mix-reconstruct paradigm. Fig. 2 provides an overview of the end-to-end pipeline. The core innovation of DecoKAN lies in replacing the conventional opaque MLP-based mixers with more expressive and interpretable Kolmogorov-Arnold Networks (KANs), performing all core mixing operations within the wavelet domain.

DecoKAN begins by robustly normalizing the input time series and then decomposing it into multiple approximation and detail coefficient series via a multi-level wavelet transform. This decomposition allows for feature extraction tailored to these decoupled components. As shown in Fig. 2 (left panel),

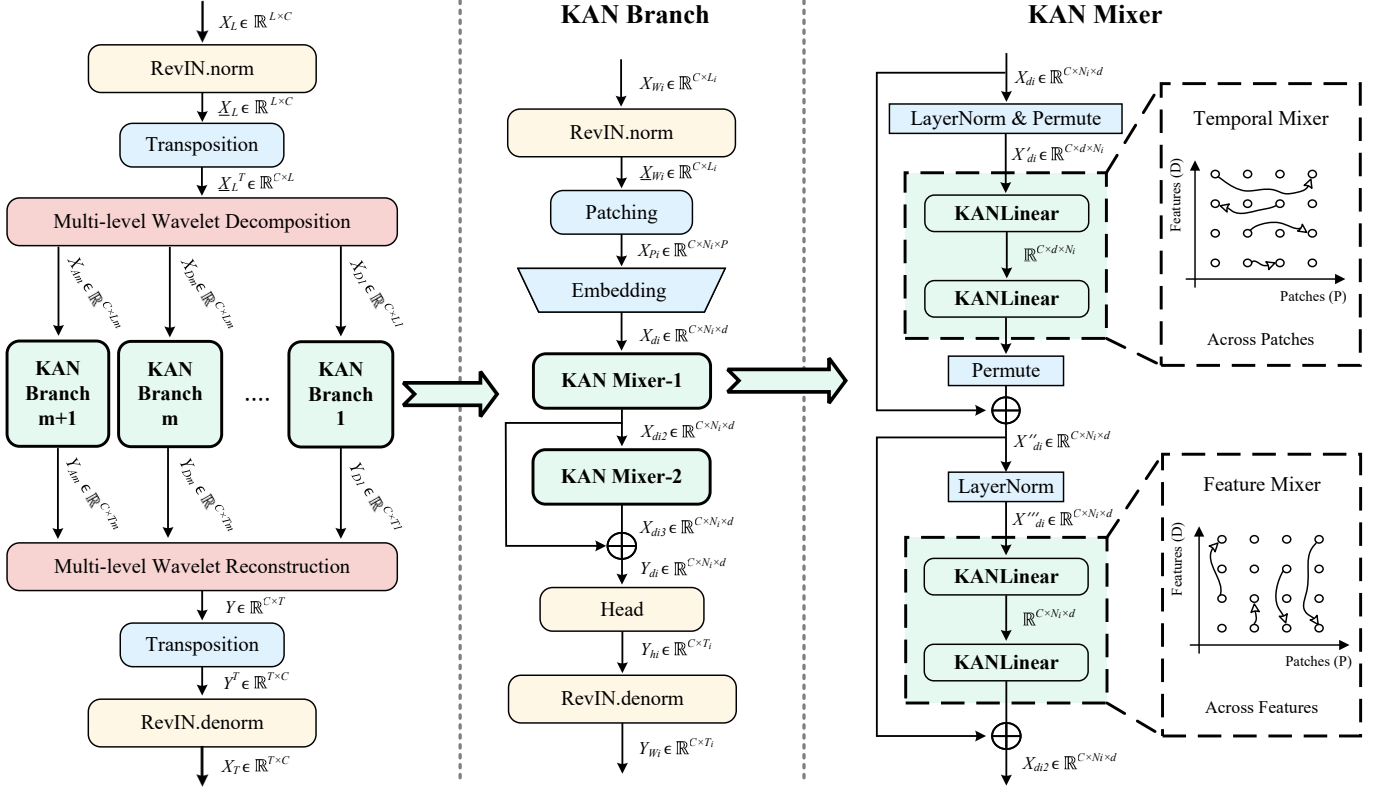


Fig. 2. Architecture overview of the proposed DecoKAN model. The model follows a decompose-mix-reconstruct paradigm: (1) Input time series is decomposed into multiple wavelet coefficient series using multi-level DWT; (2) Each coefficient series is processed by dedicated KAN Resolution Branches containing DecoKAN Mixer blocks; (3) Predicted coefficients are reconstructed back to time-domain via inverse wavelet transform.

each resulting coefficient series is then processed independently by a dedicated KAN Resolution Branch. This branch structure facilitates the parallel and independent processing of the approximation and detail components, minimizing spectral interference and enabling frequency-specific pattern learning. Within each branch (Fig. 2, middle panel), the coefficient series undergoes patching and embedding before being processed sequentially by two DecoKAN Mixer blocks. These mixers model complex temporal and feature-wise dependencies. Finally, the predicted coefficients from all branches are synthesized back into a coherent time-domain signal via an Inverse Wavelet Transform (IDWT), followed by denormalization to produce the final forecast.

B. Instance Normalization

Given the extreme volatility and non-stationarity characteristic of cryptocurrency data, mitigating distribution shift is crucial for model generalization. We employ Reversible Instance Normalization (RevIN) for this purpose, applied without learnable affine parameters consistent with our implementation [57]. As depicted in Fig. 2, RevIN normalizes the input sequence X_L by subtracting the channel-wise mean and dividing by the standard deviation before the decomposition stage, storing these statistics. Our implementation includes adding an epsilon (1e-6) to the variance and clamping the standard deviation (min 1e-4) for numerical stability. The inverse operation (RevIN.denorm) is applied after reconstruction. Normalization is also applied within each resolution

branch. The subsequent transposition $\underline{X}_L^\top \in \mathbb{R}^{C \times L}$ aligns the data tensor with the channel-first convention typically expected by DWT implementations.

C. Multi-level Wavelet Decomposition

To decompose the composite signals inherent in cryptocurrency market data—separating underlying low-frequency trends from high-frequency noise and volatility—we adopt the multi-level Discrete Wavelet Transform (DWT) approach, where the normalized, transposed time series \underline{X}_L is decomposed by iteratively applying high-pass and low-pass filters derived from the chosen wavelet basis.

We select the Daubechies 4 ('db4') wavelet, denoted by ψ , motivated by its balance between smoothness and compact support, suitable for capturing both transient and trend components in non-stationary time series. The number of decomposition levels, m , is a hyperparameter (defaulting to 1), typically chosen based on the input length L (e.g., $m \approx \lfloor \log_2 L \rfloor - k$, for a small k) and validated empirically to balance resolution and computational cost. Symmetric padding is used to handle edge effects during the DWT process. The decomposition yields $m + 1$ coefficient series:

$$[X_{A_m}, X_{D_m}, X_{D_{m-1}}, \dots, X_{D_1}] = \text{DWT}(\underline{X}_L, \psi, m) \quad (2)$$

where $X_{A_m} \in \mathbb{R}^{C \times L_m}$ is the approximation coefficient series at level m , and $X_{D_m} \in \mathbb{R}^{C \times L_m}$, ..., $X_{D_1} \in \mathbb{R}^{C \times L_1}$ are the detail coefficient series at their respective levels. Let X_{W_i}

denote one of these $m+1$ coefficient series (e.g., $X_{w_i} = X_{D_1}$ with input length $L_i = L_1$). Each $X_{w_i} \in \mathbb{R}^{C \times L_i}$ is processed by a dedicated KAN Resolution Branch.

D. KAN Branch

This section details the core processing unit of our model. Each KAN Resolution Branch first normalizes its input $X_{w_i} \in \mathbb{R}^{C \times L_i}$ using an internal RevIN.norm, producing $X_{w_i} \in \mathbb{R}^{C \times L_i}$. This normalized series then undergoes patching and embedding. The series is padded and divided into overlapping patches, creating $X_{P_i} \in \mathbb{R}^{C \times N_i \times P}$, where N_i denotes the number of patches and P denotes the patch size (with stride S). These are projected to dimension d via a shared linear layer:

$$X_{d_i} = \text{Embedding}(X_{P_i}) \in \mathbb{R}^{C \times N_i \times d} \quad (3)$$

This tensor X_{d_i} serves as the input to the first of two sequential KAN Mixer blocks and also as the starting point for a branch-level residual connection (see Fig. 2, middle panel). The data flows sequentially through the mixers:

$$X_{d_i2} = \text{KAN Mixer-1}(X_{d_i}) \quad (4)$$

$$X_{d_i3} = \text{KAN Mixer-2}(X_{d_i2}) \quad (5)$$

The final mixed representation Y_{d_i} combines the output of the second mixer with the original embedded input via this branch-level residual connection:

$$Y_{d_i} = X_{d_i} \oplus X_{d_i3} \quad (6)$$

The tensor $Y_{d_i} \in \mathbb{R}^{C \times N_i \times d}$ is the tensor finally passed to the Head module.

KAN Mixer: Each KAN Mixer block (Fig. 2, right panel) models temporal and feature interactions sequentially using KAN-based layers. It consists of two sub-modules with residual connections. The process for KAN Mixer-1 is as follows:

leftmargin=12pt, itemindent=0pt, labelsep=0.5em

- 1) **Temporal KAN Mixer:** Learns relationships along the temporal (patch, N_i) axis. The input X_{d_i} is normalized (\mathcal{N}), permuted ($\mathcal{P}_{N \leftrightarrow d}$, shape $C \times d \times N_i$), processed by the temporal KAN (KAN_p , which operates on the N_i dimension), and permuted back ($\mathcal{P}_{d \leftrightarrow N}$). This output is added to X_{d_i} via a residual connection (with Dropout, \mathcal{D}):

$$Y' = \mathcal{P}_{d \leftrightarrow N}(KAN_p(\mathcal{P}_{N \leftrightarrow d}(\mathcal{N}(X_{d_i})))) \quad (7)$$

$$X''_{d_i} = X_{d_i} + \mathcal{D}(Y') \quad (8)$$

- 2) **Feature KAN Mixer:** Captures interactions across the feature (embedding, d) dimension. The intermediate tensor X''_{d_i} is normalized, processed by the feature KAN (KAN_e , which operates on the d dimension), and added to X''_{d_i} via a second residual connection:

$$Y'' = KAN_e(\mathcal{N}(X''_{d_i})) \quad (9)$$

$$X_{d_i2} = X''_{d_i} + \mathcal{D}(Y'') \quad (10)$$

The tensor X_{d_i2} is the final output of KAN Mixer-1. KAN Mixer-2 follows the same process as KAN Mixer-1.

The advantage of these KAN-based mixers in financial modeling stems from their core KANLinear layer. Each connection uses a learnable univariate activation $\phi(x)$ (default *gridsize* = 5 and *splineorder* = 3), parameterized via B-splines over a grid, typically added to a base function $b(x)$ (SiLU in our implementation):

$$\phi(x) = w_b b(x) + w_s \sum_{j=0}^{G+k-1} c_j B_j(x) \quad (11)$$

where $B_j(x)$ are B-spline basis functions, and w_b, w_s, c_j are learnable.

Furthermore, to enhance interpretability and encourage sparsity, each KANLinear layer incorporates a regularization loss based on:

$$L_{\text{reg}} = \lambda_1 \sum_{\text{edges}} |\phi|_1 + \lambda_2 \sum_{\text{edges}} S(\phi) \quad (12)$$

This composite loss function is crucial for learning sparse and interpretable representations. It consists of two key components, balanced by internal coefficients λ_1 and λ_2 (typically set to 1.0), and weighted by an overall regularization strength hyperparameter γ (e.g., $\gamma = 1e-5$) in the total loss $L_{\text{total}} = L_{\text{forecast}} + \gamma L_{\text{reg}}$, where L_{forecast} denotes the Mean Squared Error (MSE) between the predicted and ground-truth values, and γ is a hyperparameter balancing the two terms.

leftmargin=12pt, itemindent=0pt, labelsep=0.5em

- An L1-based term $|\phi|_{avg}$ representing the average magnitude of the spline component, encouraging function sparsity.
- An entropy term $S(\phi)$ based on the normalized magnitudes (p_j) of the spline coefficients (c_j), $S(\phi) = -\sum_j p_j \log p_j$ (where $p_j = |c_j| / \sum_k |c_k|$), encouraging structural sparsity at the neuron level.

This dual-penalty regularization, controlled overall by γ , guides the model towards parsimonious and interpretable solutions during training.

E. Multi-level Wavelet Reconstruction

After the branch-level residual connection, the resulting tensor $Y_{d_i} \in \mathbb{R}^{C \times N_i \times d}$ is fed into the Head module. This module first flattens the patch and embedding dimensions using `nn.Flatten`, then uses a final `nn.Linear` layer to project the representation to the desired prediction length T_i for that specific coefficient series:

$$Y_{f_i} = \text{Flatten}(Y_{d_i}) \in \mathbb{R}^{C \times (N_i \cdot d)} \quad (13)$$

$$Y_{h_i} = \text{Linear}(Y_{f_i}) \in \mathbb{R}^{C \times T_i} \quad (14)$$

These outputs Y_{h_i} correspond to the predicted coefficients we defined earlier: $Y_{A_m} \in \mathbb{R}^{C \times T_m}$ and $Y_{D_m} \in \mathbb{R}^{C \times T_m}$, ..., $Y_{D_1} \in \mathbb{R}^{C \times T_1}$.

Finally, the Reconstruction stage synthesizes these predicted coefficients back into the time domain. The predicted approximation (Y_{A_m}) and detail (Y_{D_m}, \dots, Y_{D_1}) coefficient series from all resolution branches are combined using the inverse multi-level wavelet transform (IDWT):

$$Y = \text{IDWT}(Y_{A_m}, Y_{D_m}, \dots, Y_{D_1}) \in \mathbb{R}^{C \times T} \quad (15)$$

The resulting time series Y represents the forecast in the normalized, channel-first space. This tensor is then transposed to $Y^\top \in \mathbb{R}^{T \times C}$ and transformed using the stored RevIN parameters (denormalization) to obtain the final prediction sequence $X_T \in \mathbb{R}^{T \times C}$ in the original data space.

Algorithm 1 DecoKAN Framework: Training and Interpretation

Require: Multivariate time series \mathcal{X} , Hyperparameters (L, T, m, γ, τ)
Ensure: Trained Model θ^* , Symbolic Formulas \mathcal{F}

Phase 1: Structure-Aware Training

for epoch = 1 to E **do**

for batch (X_L, X_{true}) in DataLoader **do**

 // 1. Hierarchical Decomposition

$\tilde{X}_L \leftarrow \text{Normalize}(X_L)$

$C = [X_{A_m}, X_{D_m}, \dots, X_{D_1}] \leftarrow \text{DWT}(\tilde{X}_L, m)$

 // 2. Parallel Resolution Branch Processing

$Y_{\text{coeffs}} \leftarrow []$; $L_{\text{reg}} \leftarrow 0$

for each component c_i in C **do**

$Z_i \leftarrow \text{Embed}(c_i)$ // Implicit Patching & Normalization

$H_i \leftarrow \text{KAN_Block}(Z_i)$ // Capture non-linear patterns via Splines

$\hat{y}_i \leftarrow \text{ProjectionHead}(H_i)$

 // Sparsification via Regularization

$L_{\text{reg}} \leftarrow L_{\text{reg}} + \text{SparsityLoss}(\phi_i)$

$Y_{\text{coeffs}}.append(\hat{y}_i)$

end for

 // 3. Reconstruction & Optimization

$\hat{X}_T \leftarrow \text{Denormalize}(\text{IDWT}(Y_{\text{coeffs}}))$

$L_{\text{total}} \leftarrow \text{MSE}(\hat{X}_T, X_{\text{true}}) + \gamma \cdot L_{\text{reg}}$

 Update θ by minimizing L_{total}

end for

end for

Phase 2: Interpretability (Post-Training)

Initialize $\mathcal{F} \leftarrow \emptyset$

for each KAN layer l in optimized θ^* **do**

Pruning: Mask connections where $\|\phi_l\|_2 < \tau$

Symbolification: Extract $f_l \approx \phi_l$ maximizing R^2 and update $\mathcal{F} \leftarrow \mathcal{F} \cup \{f_l\}$

end for

return θ^* and \mathcal{F}

IV. EXPERIMENTS AND ANALYSIS

To validate the effectiveness, interpretability, and robustness of our proposed DecoKAN framework, we conducted extensive experiments across various benchmarks.

A. Experimental Setup

Datasets. Our evaluation employs a diverse set of time series datasets, encompassing both widely-adopted general benchmarks and high-volatility, real-world cryptocurrency market data, as summarized in Table I.

(1) **General Benchmarks:** For long-term forecasting, we utilize the widely-adopted ETT datasets (ETTh1, ETTh2, ETTm1, ETTm2). These datasets, collected from electricity

transformers, are commonly used to assess time series forecasting models due to their diverse temporal patterns and varying frequencies.

(2) **Cryptocurrency Benchmarks:** To rigorously test DecoKAN’s capability in its primary application domain, we introduce three real-world cryptocurrency datasets: Bitcoin (BTC), Ethereum (ETH), and Monero (XMR), sourced from the Community Network Data provided by Coin Metrics [58]. These datasets comprise comprehensive daily multivariate time series spanning diverse dimensions of the digital asset market. Key categories include market dynamics (e.g., price, market cap, volatility), on-chain activity (e.g., transaction counts, fees), and network security (e.g., hashrate, difficulty). Collectively, this rich feature set captures the complex interplay between financial sentiment, fundamental network utility, and market fundamentals, characterized by extreme volatility and complex non-stationarity.

TABLE I
DATASET STATISTICS SUMMARY

Dataset	Variates	Dataset Size	Freq.
ETTh1, ETTh2	7	(8545, 2881, 2881)	Hourly
ETTm1, ETTm2	7	(34465, 11521, 11521)	15 min
BTC	147	(6099, 4269, 1219)	Daily
ETH	146	(3700, 2590, 740)	Daily
XMR	48	(4168, 2917, 833)	Daily

Baselines. We conduct a comprehensive comparison of DecoKAN against a broad spectrum of state-of-the-art deep forecasting models, representing different architectural backbones including MLP-based, Transformer-based, CNN-based and Graph-based approaches.

MLP-based models:

- WPMixer [20] employs multi-level wavelet decomposition with MLP mixers, processing each resolution branch independently.
- TimeMixer [18] uses moving averages for seasonal-trend decomposition combined with multi-scale mixing.
- DLinear [17] is a simple linear model shown to be remarkably effective, often used as a strong baseline.

Transformer-based models:

- TimeXer [19] extends the MLP-Mixer paradigm incorporating Transformer-like elements for time series.
- PatchTST [15] applies patching to the input sequence before feeding it into a standard Transformer architecture.
- Crossformer [27] employs a two-stage attention mechanism to capture cross-time and cross-variable dependencies.

CNN-based model:

- TimesNet [21] transforms 1D time series into a 2D space based on periodicity and uses CNNs to capture variations.

Graph-based model:

- TimeFilter [35] employs a GNN-based framework with patch-specific spatial-temporal graph filtration to adaptively model fine-grained dependencies while filtering out irrelevant correlations.

Experimental Settings. To ensure a fair and reproducible comparison, our experimental setup strictly adheres to the standards established by the Time Series Library (TSLib) [21], [31]. All baseline models are evaluated using their officially reported optimal parameters. To ensure reproducibility and transparency, the detailed hyperparameter configurations for both the cryptocurrency datasets and general benchmarks are summarized in Table II. For all forecasting tasks, we employ Mean Squared Error (MSE) and Mean Absolute Error (MAE) as primary evaluation metrics. All experiments were conducted on a single NVIDIA Tesla V100 GPU.

B. Performance Comparison with Baselines

The comprehensive long-term forecasting results, comparing DecoKAN against state-of-the-art baselines across all datasets, are presented in Table III. Performance is evaluated using Mean Squared Error (MSE) and Mean Absolute Error (MAE), where lower values are better.

TABLE II
DETAILED HYPERPARAMETER CONFIGURATIONS FOR DEOKAN.
VALUES INCLUDE THE CANDIDATE SEARCH SPACES AND RANGES
EXPLORED DURING OPTIMIZATION.

Parameter	Crypto Benchmarks	ETT Benchmarks
Look-back Window (L)	96 {24, 48, 96, 168}	512 {96, 192, 336, 720}
Wavelet Basis (ψ)	db4	db2 / db4
Decomposition Level (m)	1, 2	1, 2, 3
KAN Grid Size (G)	5	5
KAN Spline Order (k)	3	3
Patch Size (P)	8, 16	16, 48
Patch Stride (S)	4, 8	8, 24
Model Dimension (d)	64, 128, 256	64, 128
Temporal Factors	2 ~ 6	2 ~ 6
Dimension Factors	2 ~ 6	2 ~ 8
Dropout Rate	0.05 ~ 0.3	0.0 ~ 0.4
Batch Size	4, 8, 16	32, 64, 128
Learning Rate	$1e^{-4} \sim 5e^{-4}$	$1e^{-4} \sim 1e^{-3}$
epochs	30	30, 50

TABLE III

EXPERIMENTAL RESULTS ON LONG-TERM TIME SERIES FORECASTING. RESULTS ARE REPORTED AS MSE/MAE. BEST RESULTS ARE IN **BOLD**, SECOND-BEST ARE UNDERLINED. THE LENGTH OF THE LOOK-BACK WINDOW IS A HYPERPARAMETER.

Models	DecoKAN (Ours)		WPMixer AAAI'25		TimeFilter ICML'25		TimeMixer ICLR'24		TimeXer NeurIPS'24		TimesNet ICLR'23		PatchTST ICLR'23		DLinear AAAI'23		Crossformer ICLR'23		
Metric	MSE	MAE	MSE	MAE	MSE	MAE	MSE	MAE	MSE	MAE	MSE	MAE	MSE	MAE	MSE	MAE	MSE	MAE	
ETTh1	96	0.370	0.399	0.371	0.399	0.389	0.399	0.375	0.397	0.383	0.403	0.407	0.425	0.382	0.400	0.396	0.411	0.451	0.455
	192	0.406	<u>0.418</u>	0.432	0.440	0.440	0.427	<u>0.429</u>	0.427	0.442	0.438	0.465	0.460	0.430	0.433	0.447	0.443	0.477	0.476
	336	0.439	<u>0.444</u>	0.441	0.450	0.478	<u>0.445</u>	0.481	<u>0.451</u>	0.483	0.452	0.496	0.471	0.472	0.460	0.496	0.473	0.572	0.530
	720	0.436	<u>0.460</u>	0.489	0.486	0.507	0.482	0.490	<u>0.476</u>	0.520	0.494	0.513	0.495	0.513	0.501	0.510	0.508	0.913	0.743
	Avg	0.413	<u>0.430</u>	0.433	0.444	0.454	<u>0.438</u>	0.444	<u>0.438</u>	0.457	0.447	0.471	0.463	0.449	0.448	0.462	0.459	0.603	0.551
ETTh2	96	0.278	<u>0.341</u>	0.281	0.348	0.287	0.337	0.291	<u>0.341</u>	0.283	0.337	0.345	0.381	0.304	0.353	0.350	0.402	0.635	0.555
	192	0.365	0.396	<u>0.368</u>	0.402	0.376	0.394	0.373	0.393	0.368	0.393	0.423	0.417	0.379	0.400	0.463	0.469	0.578	0.548
	336	0.373	<u>0.404</u>	0.381	0.420	0.430	0.439	0.437	0.433	0.434	0.438	0.444	0.453	0.400	0.452	0.573	0.533	0.896	0.669
	720	0.402	0.439	0.395	<u>0.437</u>	0.447	0.458	0.437	0.448	0.445	0.454	0.455	0.465	0.456	0.464	0.839	0.661	1.097	0.757
	Avg	0.354	<u>0.395</u>	0.357	0.402	0.385	0.407	0.385	0.404	0.383	0.406	0.417	0.429	0.385	0.417	0.556	0.516	0.802	0.632
ETTm1	96	0.303	0.354	0.300	<u>0.349</u>	0.320	0.359	0.318	0.358	0.322	0.359	0.328	0.369	0.324	0.364	0.345	0.372	0.403	0.412
	192	<u>0.337</u>	0.374	0.336	<u>0.371</u>	0.362	0.381	0.360	0.380	0.365	0.385	0.411	0.407	0.370	0.390	0.382	0.390	0.477	0.458
	336	0.369	0.399	0.372	0.390	0.391	0.403	0.385	0.400	0.401	0.409	0.423	0.426	0.398	0.409	0.415	0.414	0.474	0.472
	720	0.421	<u>0.417</u>	0.435	0.423	0.460	0.438	0.454	0.442	0.453	0.441	0.493	0.463	0.464	0.447	0.472	0.450	0.532	0.503
	Avg	0.358	0.386	0.361	0.383	0.383	0.395	0.379	0.395	0.385	0.399	0.414	0.416	0.389	0.402	0.403	0.407	0.472	0.461
ETTm2	96	0.170	0.261	0.168	<u>0.257</u>	0.173	0.259	0.176	<u>0.258</u>	0.171	0.257	0.185	0.264	0.180	0.265	0.194	0.293	0.285	0.370
	192	0.228	<u>0.298</u>	0.232	0.305	0.237	0.300	0.242	<u>0.302</u>	0.240	0.301	0.256	0.310	0.247	0.311	0.284	0.361	0.388	0.438
	336	0.276	<u>0.330</u>	0.277	<u>0.331</u>	0.296	0.338	0.305	0.346	0.297	0.339	0.314	0.345	0.314	0.352	0.373	0.421	0.613	0.541
	720	0.381	<u>0.396</u>	0.413	0.411	0.397	<u>0.398</u>	0.396	0.400	<u>0.394</u>	0.396	0.421	0.409	0.421	0.415	0.538	0.515	1.356	0.785
	Avg	0.264	<u>0.321</u>	0.272	0.326	0.276	0.324	0.280	0.327	0.275	<u>0.323</u>	0.294	0.332	0.290	0.336	0.347	0.398	0.661	0.534
BTC	24	0.108	0.096	0.134	0.133	0.110	0.106	0.146	0.112	0.108	0.101	0.138	0.135	0.107	0.098	0.109	0.115	0.145	0.167
	48	0.120	0.115	0.153	0.152	0.121	0.116	0.131	0.123	0.119	0.119	0.141	0.146	0.118	0.116	0.123	0.145	0.186	0.210
	96	0.142	<u>0.138</u>	0.163	0.168	0.158	<u>0.142</u>	0.160	0.154	0.143	0.145	0.166	0.168	0.144	0.146	0.156	0.188	0.221	0.245
	168	0.174	0.172	0.190	0.192	0.193	0.175	0.172	<u>0.166</u>	0.178	0.177	0.210	0.213	0.181	0.177	0.198	0.227	0.293	0.309
	Avg	0.136	<u>0.130</u>	0.160	0.161	0.146	0.135	0.152	0.139	<u>0.137</u>	0.135	0.164	0.166	0.137	0.134	0.146	0.169	0.211	0.233
ETH	24	0.061	<u>0.108</u>	0.110	0.174	0.078	0.121	0.072	0.114	0.064	0.114	0.109	0.174	0.062	0.112	<u>0.062</u>	0.128	0.088	0.171
	48	0.084	<u>0.136</u>	0.133	0.195	0.097	0.144	0.099	0.145	0.091	0.143	0.129	0.193	0.088	0.143	<u>0.089</u>	0.169	0.107	0.190
	96	0.110	<u>0.169</u>	0.153	0.220	0.128	0.172	0.136	0.188	0.115	0.173	0.158	0.223	0.114	0.179	0.126	0.229	0.154	0.260
	168	0.144	0.205	0.168	0.242	0.167	<u>0.203</u>	0.168	0.219	0.177	0.223	0.205	0.261	0.147	0.198	0.181	0.304	0.198	0.317
	Avg	0.100	<u>0.155</u>	0.141	0.208	0.118	<u>0.160</u>	0.119	0.166	0.112	0.163	0.150	0.213	<u>0.103</u>	0.162	0.115	0.208	0.137	0.234
XMR	24	0.142	<u>0.112</u>	0.189	0.153	0.165	0.113	0.143	0.109	0.144	0.114	0.210	0.158	0.284	0.143	0.141	0.117	0.157	0.165
	48	0.185	<u>0.139</u>	0.239	0.177	0.190	0.140	<u>0.186</u>	0.137	0.199	0.148	0.273	0.184	0.382	0.183	0.192	0.160	0.193	0.190
	96	0.239	<u>0.175</u>	0.279	0.202	0.262	0.172	0.261	0.177	0.253	0.178	0.297	0.210	0.576	0.236	0.254	0.211	0.241	0.214
	168	0.310	<u>0.215</u>	0.324	0.227	0.326	<u>0.216</u>	0.336	0.224	<u>0.313</u>	0.217	0.364	0.257	0.580	0.253	0.330	0.248	0.325	0.279
	Avg	0.219	<u>0.160</u>	0.258	0.190	0.235	0.160	0.231	<u>0.162</u>	0.227	0.164	0.286	0.202	0.455	0.204	0.229	0.184	0.229	0.212
1stCount:	27	21	4	6	0	3	1	5	0	4	0	0	2	1	1	0	0	0	

On the general ETT benchmark datasets, DecoKAN demonstrates strong performance. It achieves the best overall average MSE and MAE on the ETTh1 dataset, reducing average MSE by approximately 4.6% compared to the next best model, WPMixer. On ETTh2 and ETM2, DecoKAN also yields the lowest average MSE among all models considered. While WPMixer shows a marginally better average MAE on ETM1, DecoKAN maintains competitive accuracy across most prediction horizons, particularly for longer-term forecasts (e.g., $T = 720$) on ETTh1 and ETTh2, underscoring the robustness of the wavelet-KAN architecture.

Notably, this solid performance translates into leading results on the highly volatile cryptocurrency datasets (BTC, ETH, XMR), which represent our primary application domain. DecoKAN achieves the lowest average MSE and MAE across all horizons for all three cryptocurrency datasets compared to all baselines listed in Table III. Specifically, compared to the recent WPMixer baseline, DecoKAN reduces the average MSE by approximately 15.0% on BTC, 29.1% on ETH, and 15.1% on XMR. Furthermore, even against the state-of-the-art graph-based model TimeFilter, DecoKAN maintains a distinct advantage, achieving an overall average MSE reduction of 9.6% across these cryptocurrency datasets. Notably compared to the closest competitors like PatchTST on BTC/ETH or TimeXer on XMR, DecoKAN consistently maintains an edge in average MSE.

This observed advantage in the target domain aligns with our design principles. We attribute this effective performance primarily to DecoKAN’s architectural strengths: the multi-level wavelet decomposition effectively disentangles the high-frequency market noise characteristic of cryptocurrencies from their underlying long-term trends. Subsequently, the KAN-based mixers, with their ability to learn explicit non-linear functions, can model the complex dynamics within these separated components more effectively than traditional MLP or attention mechanisms, which may struggle with the extreme volatility and non-stationarity of crypto data. The results validate that DecoKAN offers an effective integration of signal processing and interpretable deep learning for addressing challenging real-world forecasting tasks.

C. Computational Efficiency Analysis

The previous section examined DecoKAN’s forecasting accuracy. To evaluate its practicality for real-world deployment, we analyze its efficiency from four complementary perspectives: parameter count, theoretical computation (GFLOPs), empirical training speed, and inference latency. All comparisons are conducted on the ETTh1 dataset ($L = 96$) under unified configurations ($d_{model} = 16$, Batch = 64, $d_{ff} = 4 \times d_{model}$) to ensure fairness. The results are summarized in Fig. 3.

Parameter Count. DecoKAN’s parameter count ranges from 0.11M to 0.18M across different prediction horizons. This is broadly comparable to other MLP-based architectures such as WPMixer (0.09M–0.16M) and TimeMixer (0.08M–0.19M). The modest increase compared to the minimal PatchTST model follows naturally from the use of B-spline coefficients in the KANLinear layers, which introduce

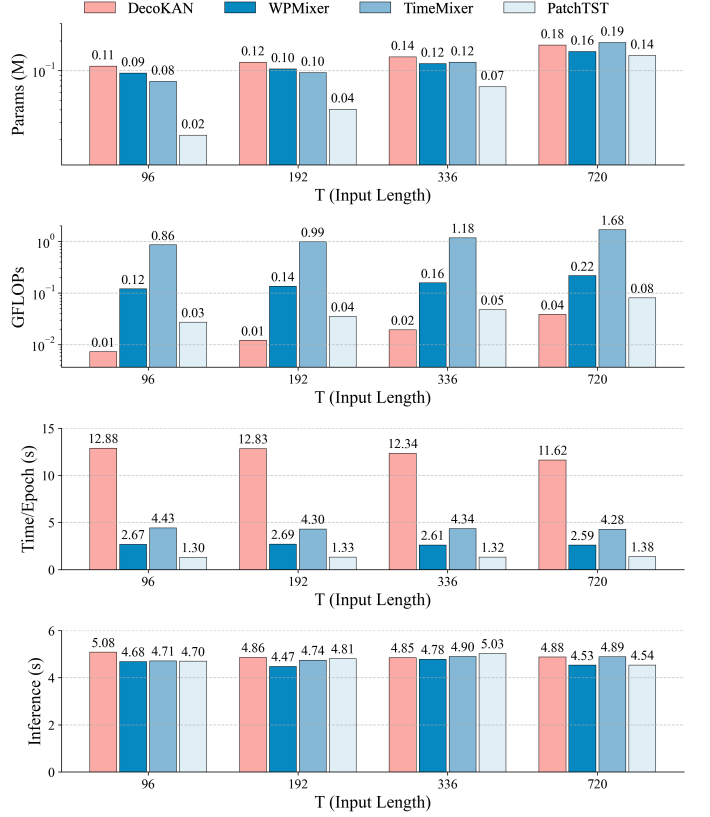


Fig. 3. Computational efficiency comparison on the ETTh1 dataset ($L = 96$). The plots illustrate (from top to bottom): total parameter count (M), theoretical computation in GFLOPs (log scale), empirical training time per epoch (s), and inference time (s) for various prediction lengths (T).

additional learnable parameters per connection to enable flexible non-linear modeling capabilities.

Computation complexity (GFLOPs). In terms of theoretical computational complexity, DecoKAN demonstrates exceptional efficiency. It achieves the lowest GFLOPs across all settings; for instance, at $T = 96$, its 0.0073 GFLOPs is approximately 16 times lower than WPMixer (0.12) and orders of magnitude lower than TimeMixer (0.86). This highlights the intrinsic efficiency of the sparse KAN architecture in representing complex functions with fewer floating-point operations compared to dense MLP computations.

Training Time. Despite its low theoretical cost, DecoKAN exhibits the longest empirical training time. At $T = 96$, each epoch takes approximately 12.6 seconds, which is about 4.9 times slower than WPMixer (≈ 2.5 s) and nearly 10 times slower than PatchTST (≈ 1.3 s). This discrepancy stems from the current implementation of B-spline computations, which are memory-intensive and less optimized for parallel GPU execution compared to the highly optimized dense matrix multiplications central to standard MLPs and Transformers.

Inference Time. Crucially for deployment, the inference latency of DecoKAN remains highly competitive. The inference time for the full test set (e.g., ≈ 5.1 s at $T = 96$) is nearly identical to that of the baseline models, such as WPMixer (4.7s) and PatchTST (4.7s). This indicates that the computational overhead is primarily confined to the training

phase and does not hinder the model's efficiency during real-time forecasting applications. Nevertheless, the results confirm that the computational overhead is strictly confined to the offline training phase and does not hinder the model's efficiency during real-time forecasting applications.

Summary. The comprehensive efficiency analysis reveals that DecoKAN embodies a distinct computational trade-off. While it incurs higher training costs due to the current lack of hardware optimization for B-spline computations, this investment yields significant returns in forecasting accuracy (Sec. 4.2) and intrinsic symbolic interpretability (Sec. 5). Most importantly, DecoKAN's exceptionally low theoretical complexity translates into inference speeds that are fully viable for real-time deployment in high-frequency trading systems.

D. Ablation Study

To quantitatively validate the contribution of the core KAN components within the DecoKAN framework, we conducted a comprehensive ablation study on both a general benchmark (ETTh2) and a target-domain dataset (ETH). We tested the following four model configurations:

- **Full KAN:** The complete model, utilizing KANs for both temporal and feature mixing.
- **Temporal KAN only:** A variant where the Feature KAN mixer is replaced by a standard MLP, isolating the contribution of the temporal mixing component.
- **Feature KAN only:** A variant where the Temporal KAN mixer is replaced by an MLP, isolating the contribution of the feature mixing component.
- **Baseline (MLP only):** A variant where KAN mixers are replaced by standard MLPs while preserving DecoKAN's exact backbone and hyperparameters. Note that this internal baseline is architecturally distinct from the WPMixer [20] model, designed specifically here to strictly isolate the contribution of the KAN mechanism.

For each configuration, we conducted five independent runs using different random seeds to ensure the robustness of our findings. The distribution of the total average Mean Squared Error (MSE) for each case is presented in the box plots in Fig. 4.

Analysis of ETTh2 Dataset: On the ETTh2 dataset, the results (Fig. 4, left panel) show a general performance hierarchy. The Full DecoKAN model achieves the lowest average MSE. Removing either the temporal KAN (Temporal KAN only) or the feature KAN (Feature KAN only) component leads to a noticeable increase in average MSE, with both variants performing similarly to each other but worse than the full model. The Baseline (MLP only) model yields the highest average MSE. Since this baseline shares the identical decomposition structure as DecoKAN, this performance gap directly validates the superior modeling capability of KAN mixers over standard MLPs, independent of the wavelet framework itself. This validates that for a general, seasonal time series like ETTh2, both the temporal and feature KAN components contribute positively to achieving optimal performance.

Analysis of ETH Dataset: Notably, the ablation study on the volatile ETH dataset reveals a different dynamic (Fig. 4,

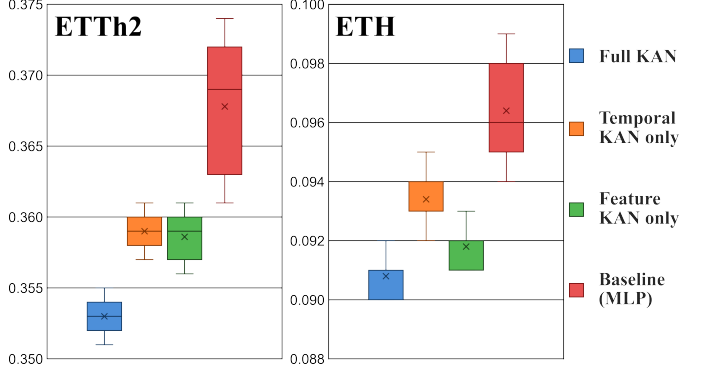


Fig. 4. Ablation study results on the ETTh2 and ETH datasets. Each box plot shows the distribution of average MSE over 5 independent runs with different random seeds. The 'x' marks the mean performance. Lower values indicate better performance, and a smaller box indicates higher stability.

right panel). The performance distribution of Feature KAN only closely matches that of the Full DecoKAN model, indicating similar average MSE and variance across runs. In contrast, the Temporal KAN only configuration exhibits a clear increase in average MSE compared to the Full DecoKAN. The Baseline (MLP only) configuration yields the highest average MSE among the tested variants on this dataset as well.

This distinct behavior aligns with the inherent characteristics of cryptocurrency markets. Unlike traditional time series (e.g., electricity load) dominated by strong temporal autocorrelation, cryptocurrency prices are often driven by high-frequency shocks and the instantaneous interplay between system variables (e.g., the non-linear coupling between trading volume, transaction fees, and price volatility). Consequently, the performance of DecoKAN here relies predominantly on the Feature KAN component's ability to capture these complex cross-variate dependencies, proving more critical than the temporal mixing for this domain. This indicates DecoKAN can adapt the relative importance of its internal components based on data characteristics. Furthermore, the observed performance difference between the KAN-based configurations and the MLP baseline, coupled with DecoKAN's intrinsic interpretability (as demonstrated in Section 4.5), underscores its advantages for trustworthy forecasting in critical financial applications.

The compact nature of the box plots across both datasets also visually confirms the stability and robustness of the DecoKAN architecture against random initializations.

E. Interpretability Analysis

A core advantage of DecoKAN is its intrinsic interpretability. This is realized by leveraging the three-stage pipeline native to Kolmogorov-Arnold Networks conceptually illustrated in Fig. 5—Sparsification, Pruning, and Symbolification—which allows transforming the trained network's learnable activation functions into concise, mathematically explicit symbolic formulas. Sparsification is achieved during training via the regularization loss L_{reg} (Eq. 12), encouraging parsimonious solutions. This section presents a case study on the ETH price prediction task to demonstrate how subsequent

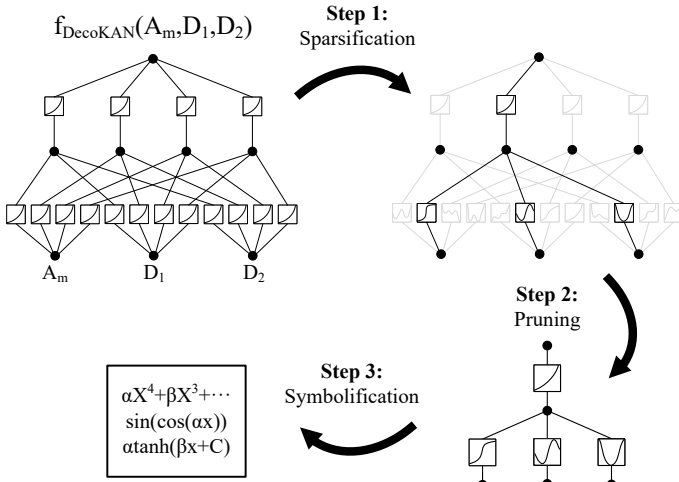


Fig. 5. An example of how to do symbolic regression with KAN. Steps 1–3 correspond to Lines 21, 34, 35 of Algorithm 1 respectively.

Pruning and Symbolification reveal the internal functional specialization of the DecoKAN framework.

TABLE IV

PRUNING STATISTICS OF DECOKAN ON THE ETH DATASET ($\tau = 0.05$). VALUES DENOTE THE COUNT OF LEARNABLE EDGES.

Branch	Total	Pruned	Preserved	Prune Ratio
Approximation	12,720	609	12,111	4.79%
Detail	12,720	9,703	3,017	76.28%
Overall Model	25,440	10,312	15,128	40.53%

For this case study, we employ a single-level wavelet decomposition ($m = 1$). This configuration simplifies the model into two distinct processing pathways, each with a dedicated KAN Resolution Branch:

- **Approximation Branch**, processing the low-frequency approximation coefficients (A_1) related to the underlying trend.
- **Detail Branch**, processing the high-frequency detail coefficients (D_1) related to volatility and noise components.

Following sparsification-guided training, the network is

pruned by removing connections whose spline activation function's L2 norm falls below a threshold τ (set to 0.05 in this study). Table IV summarizes the pruning status for the two branches, revealing their structural efficiency.

The pruning results in Table IV highlight a clear functional specialization. The Approximation Branch exhibits a low pruning ratio of only 4.79%, signifying that its connections are fundamental and highly efficient, forming an indispensable structural backbone for preserving the low-frequency components of the ETH prices. Conversely, the Detail Branch shows a much higher pruning ratio of 76.28%, indicating a high degree of learned sparsity. This suggests that while the branch begins with high capacity, it effectively selects only the most critical connections to model the transient fluctuations.

Finally, symbolification replaces the remaining B-spline activation functions in the pruned network with mathematically explicit symbolic formulas, selected based on the best fit (R^2) from a candidate library (e.g., polynomials, trigonometric). To demonstrate the model's capability to discover explicit physical dynamics from data, Table V lists the top symbolic functional relationships discovered by the DecoKAN model on the ETH dataset, rigorously ranked by their coefficient of determination (R^2).

This detailed symbolic analysis corroborates the functional specialization observed during pruning, revealing three critical insights within a unified view. First, the consistently high R^2 scores (predominantly > 0.99) across the top rankings validate the KAN mixers' convergence to precise functional mappings. Second, the Detail Branch overwhelmingly dominates these rankings with complex polynomial and trigonometric formulas (e.g., Rank 3), providing explicit mathematical explanations for high-frequency market volatility. In contrast, the Approximation Branch appears sparsely in this high-confidence symbolic list (represented solely by Rank 9). This scarcity aligns with our pruning analysis, suggesting that the Approximation Branch functions primarily as a stable, dense structural backbone that preserves low-frequency components through distributed weights rather than relying on specific symbolic curve-fitting.

In summary, the interpretability analysis validates DecoKAN's design, revealing a clear functional division: the Approximation Branch provides a robust structural backbone

TABLE V

TOP SYMBOLIC FORMULAS EXTRACTED FROM KAN MIXER CONNECTIONS ON ETH DATASET (RANKED BY R^2 SCORE) (LAYER I AND LAYER J DENOTE THE INPUT AND OUTPUT NODE INDICES OF THE RESPECTIVE KAN LINEAR LAYER WITHIN THE SPECIFIED MIXER BLOCK)

Branch	KAN Mixer	Layer <i>i</i>	Layer <i>j</i>	Symbolic Formula	R^2 Score
Detail Branch	KAN Mixer 2	120	15	$-0.076x^4 + 0.216x^3 + 0.252x^2 - 1.370x - 0.116$	0.9968
Detail Branch	KAN Mixer 1	126	8	$-0.153x^4 + 0.170x^3 + 0.610x^2 - 1.270x - 0.334$	0.9958
Detail Branch	KAN Mixer 1	111	2	$-1.403 \sin(0.905x + 0.039) - 0.156 \cos(2.721x)$	0.9941
Detail Branch	KAN Mixer 1	43	26	$-1.307 \sin(1.072x + 0.056) - 0.186 \cos(-3.039x)$	0.9937
Detail Branch	KAN Mixer 1	20	72	$-0.047x^4 + 0.226x^3 + 0.080x^2 - 1.386x + 0.004$	0.9931
Detail Branch	KAN Mixer 2	36	11	$0.163x^4 - 0.195x^3 - 0.596x^2 + 1.317x + 0.302$	0.9926
Detail Branch	KAN Mixer 1	8	4	$-1.282 \tanh(1.431x + 0.029)$	0.9905
Detail Branch	KAN Mixer 1	72	2	$0.112x^4 - 0.144x^3 - 0.390x^2 + 1.240x + 0.189$	0.9884
Approx Branch	KAN Mixer 2	26	4	$0.923 \sin(1.348x + 0.695) + 0.801 \cos(2.624x)$	0.9862
Detail Branch	KAN Mixer 1	23	1	$1.044 \sin(1.312x + 0.462) + 0.678 \cos(2.631x)$	0.9826

for the forecasting task, while the Detail Branch acts as a high-capacity engine for capturing complex volatility dynamics.

V. CONCLUSION

This paper presents DecoKAN, a framework combining multi-resolution wavelet decomposition (DWT) with the intrinsic interpretability of Kolmogorov–Arnold Networks (KANs) to generate explicit mathematical laws from data for multivariate time series forecasting in cryptocurrency systems. Through extensive experiments, DecoKAN demonstrated competitive predictive accuracy and improvements in forecasting volatile cryptocurrency markets. Interpretability analysis revealed a functional separation within the model: the Detail Branch captures explicit symbolic relations for high-frequency fluctuations, while the Approximation Branch acts as a robust structural backbone for the forecasting task.

However, limitations remain. A primary constraint is computational efficiency. KANs rely on B-spline computations that are currently less optimized for GPU parallelization, leading to slower training times compared to MLP or Transformer-based architectures. Crucially, however, this overhead is confined to training; our experiments confirm that DecoKAN’s inference latency remains highly competitive, ensuring its practical viability for real-time deployment. Additionally, the symbolification process depends on a finite set of candidate functions, and interpreting the resulting symbolic graphs requires human domain expertise.

Future work will address these challenges. Methodologically, we aim to bridge the training efficiency gap by incorporating recent advances in efficient KAN implementations, such as CUDA-accelerated grids and network quantization, to significantly reduce overhead without compromising interpretability. Architecturally, integrating KAN modules into other forecasting backbones may enable new interpretable models for time series. In applications, DecoKAN’s transparency makes it suitable for analyzing collective market behavior and social sentiment dynamics, including market manipulation detection, algorithmic trading, and risk assessment in DeFi.

REFERENCES

- [1] S. Werner, D. Perez, L. Gudgeon, A. Klages-Mundt, D. Harz, and W. J. Knottenbelt, “SoK: Decentralized finance (DeFi),” in *Proceedings of the 4th ACM Conference on Advances in Financial Technologies (AFT ’22)*, Sep. 2022, pp. 30–46.
- [2] S. Corbet, Y. Hou, Y. Hu, C. Larkin, B. Lucey, and L. Oxley, “Cryptocurrency liquidity and volatility interrelationships during the COVID-19 pandemic,” *Finance Research Letters*, vol. 45, p. 102137, Mar. 2022.
- [3] Y. Zhang, Z. Li, Y. Su, J. Li, and S. Chen, “A novel method for bitcoin price manipulation identification based on graph representation learning,” *IEEE Transactions on Computational Social Systems*, vol. 11, no. 5, pp. 5607–5618, 2024.
- [4] G. E. P. Box, G. M. Jenkins, G. C. Reinsel, and G. M. Ljung, *Time Series Analysis: Forecasting and Control*. John Wiley & Sons, 2015.
- [5] M. R. Hassan and B. Nath, “Stock market forecasting using hidden Markov model: a new approach,” in *Proceedings of the 5th International Conference on Intelligent Systems Design and Applications (ISDA)*, Sep. 2005.
- [6] P. Katsiampa, “Volatility estimation for Bitcoin: A comparison of GARCH models,” *Economics Letters*, vol. 158, pp. 3–6, 2017.
- [7] M. Liu et al., “SCINet: Time series modeling and forecasting with sample convolution and interaction,” in *Advances in Neural Information Processing Systems*, vol. 35, 2022, pp. 5816–5828.
- [8] A. Vaswani et al., “Attention is all you need,” in *Advances in Neural Information Processing Systems*, vol. 30, 2017, pp. 5998–6008.
- [9] H. Zhou et al., “Informer: Beyond efficient transformer for long sequence time-series forecasting,” in *Proceedings of the AAAI Conference on Artificial Intelligence*, vol. 35, no. 12, May 2021, pp. 11106–11115.
- [10] H. Wu, J. Xu, J. Wang, and M. Long, “Autoformer: Decomposition transformers with auto-correlation for long-term series forecasting,” in *Advances in Neural Information Processing Systems*, vol. 34, 2021, pp. 22419–22430.
- [11] T. Zhou, Z. Ma, Q. Wen, X. Wang, L. Sun, and R. Jin, “Fedformer: Frequency enhanced decomposed transformer for long-term series forecasting,” in *Proceedings of the International Conference on Machine Learning*, ser. Proceedings of Machine Learning Research, 2022, pp. 27268–27286.
- [12] Y. Liu, H. Wu, J. Wang, and M. Long, “Non-stationary transformers: Exploring the stationarity in time series forecasting,” in *Advances in Neural Information Processing Systems*, vol. 35, 2022, pp. 9881–9896.
- [13] R. Chiong, Z. Fan, Z. Hu, and S. Dhakal, “A novel ensemble learning approach for stock market prediction based on sentiment analysis and the sliding window method,” *IEEE Transactions on Computational Social Systems*, vol. 10, no. 5, pp. 2613–2623, 2023.
- [14] V. Gurgul, S. Lessmann, and W. K. Härdle, “Deep learning and NLP in cryptocurrency forecasting: Integrating financial, blockchain, and social media data,” *International Journal of Forecasting*, vol. 41, no. 4, pp. 1666–1695, 2025.
- [15] Y. Nie, N. H. Nguyen, P. Sinthong, and J. Kalagnanam, “A time series is worth 64 words: Long-term forecasting with transformers,” in *Proceedings of the International Conference on Learning Representations*, 2023.
- [16] Y. Liu et al., “iTTransformer: Inverted transformers are effective for time series forecasting,” in *Proceedings of the International Conference on Learning Representations*, 2023.
- [17] A. Zeng, M. Chen, L. Zhang, and Q. Xu, “Are transformers effective for time series forecasting?” in *Proceedings of the AAAI Conference on Artificial Intelligence*, vol. 37, no. 9, Jun. 2023, pp. 11121–11128.
- [18] S. Wang et al., “Timemixer: Decomposable multiscale mixing for time series forecasting,” in *Proceedings of the International Conference on Learning Representations*, 2023.
- [19] S.-A. Chen, C.-L. Li, N. Yoder, S. O. Arik, and T. Pfister, “TSMixer: An all-MLP architecture for time series forecasting,” *arXiv preprint arXiv:2303.06053*, Sep. 2023.
- [20] M. M. N. Murad, M. Aktukmak, and Y. Yilmaz, “WPMixer: Efficient multi-resolution mixing for long-term time series forecasting,” in *Proceedings of the AAAI Conference on Artificial Intelligence*, vol. 39, no. 18, Apr. 2025, pp. 19581–19588.
- [21] H. Wu, T. Hu, Y. Liu, H. Zhou, J. Wang, and M. Long, “TimesNet: Temporal 2D-variation modeling for general time series analysis,” in *Proceedings of the International Conference on Learning Representations*, 2023.
- [22] Y. Wang, H. Wu, J. Dong, G. Qin, H. Zhang, Y. Liu, Y. Qiu, J. Wang, and M. Long, “TimeXer: Empowering transformers for time series forecasting with exogenous variables,” in *Advances in Neural Information Processing Systems*, vol. 37, 2024, pp. 9014–9039.
- [23] I. Tolstikhin et al., “MLP-Mixer: An all-MLP architecture for vision,” in *Advances in Neural Information Processing Systems*, vol. 34, 2021, pp. 24261–24272.
- [24] Z. Liu et al., “KAN: Kolmogorov-arnold networks,” in *Proceedings of the International Conference on Learning Representations*, 2025.
- [25] Z. Liu, P. Ma, Y. Wang, W. Matusik, and M. Tegmark, “KAN 2.0: Kolmogorov-arnold networks meet science,” *arXiv preprint arXiv:2408.10205*, 2024.
- [26] T. Rojat, R. Puget, D. Filliat, J. D. Ser, R. Gelin, and N. Díaz-Rodríguez, “Explainable artificial intelligence (XAI) on time-series data: A survey,” *arXiv preprint arXiv:2104.00950*, Apr. 2021.
- [27] Y. Zhang and J. Yan, “Crossformer: Transformer utilizing cross-dimension dependency for multivariate time series forecasting,” in *Proceedings of the International Conference on Learning Representations*, 2023.
- [28] D. Salinas, V. Flunkert, J. Gasthaus, and T. Januschowski, “Deepar: Probabilistic forecasting with autoregressive recurrent networks,” *International Journal of Forecasting*, vol. 36, no. 3, pp. 1181–1191, 2020. [Online]. Available: <https://www.sciencedirect.com/science/article/pii/S0169207019301888>
- [29] D. Cao, F. Jia, S. O. Arik, T. Pfister, Y. Zheng, W. Ye, and Y. Liu, “TEMPO: Prompt-based generative pre-trained transformer for time series forecasting,” in *Proceedings of the Twelfth International Conference on Learning Representations*, 2024.

[30] X. Kong et al., "Deep learning for time series forecasting: A survey," *International Journal of Machine Learning and Cybernetics*, 2025.

[31] Y. Wang, H. Wu, J. Dong, Y. Liu, M. Long, and J. Wang, "Deep time series models: A comprehensive survey and benchmark," *arXiv preprint arXiv:2407.13278*, 2024.

[32] K. Yi, Q. Zhang, W. Fan, S. Wang, P. Wang, H. He, N. An, D. Lian, L. Cao, and Z. Niu, "Frequency-domain MLPs are more effective learners in time series forecasting," in *Proceedings of the 37th International Conference on Neural Information Processing Systems*, ser. NIPS '23. Red Hook, NY, USA: Curran Associates Inc., 2023.

[33] G. Woo, C. Liu, D. Sahoo, A. Kumar, and S. C. H. Hoi, "Etsformer: Exponential smoothing transformers for time-series forecasting," *arXiv preprint arXiv:2202.01381*, 2022.

[34] A. Das, W. Kong, A. Leach, S. K. Mathur, R. Sen, and R. Yu, "Long-term forecasting with TiDE: Time-series dense encoder," *Transactions on Machine Learning Research*, 2023.

[35] Y. Hu, G. Zhang, P. Liu, D. Lan, N. Li, D. Cheng, T. Dai, S.-T. Xia, and S. Pan, "Timefilter: Patch-specific spatial-temporal graph filtration for time series forecasting," in *Proceedings of the International Conference on Machine Learning*, 2025. [Online]. Available: <https://openreview.net/forum?id=pcbC3aQB5W>

[36] T. Liu et al., "The role of transformer models in advancing blockchain technology: A systematic survey," *arXiv preprint arXiv:2409.02139*, 2024.

[37] J. Wu, W. Zhang, Y. Liu, Y. Wang, Y. Zhang, and B. Yin, "Multi-attributesd: An adaptive self-knowledge distillation method for financial time series prediction," *IEEE Transactions on Computational Social Systems*, pp. 1–15, 2025.

[38] R. Gençay, F. Selçuk, and B. J. Whitcher, *An Introduction to Wavelets and Other Filtering Methods in Finance and Economics*. Elsevier, 2001.

[39] R. Mousa, M. Afrookhteh, H. Khaloo, B. A. Ali, and G. Heidary, "Forecasting of Bitcoin prices using hashrate features: Wavelet and deep stacking approach," *arXiv preprint arXiv:2501.13136*, 2025.

[40] T. Kikuchi, "Wavelet analysis of cryptocurrencies: Non-linear dynamics in high frequency domains," *arXiv preprint arXiv:2411.14058*, 2024.

[41] X. Yu, Z. Chen, Y. Ling, S. Dong, Z. Liu, and Y. Lu, "Temporal data meets LLM-explainable financial time series forecasting," *arXiv preprint arXiv:2306.11025*, 2023.

[42] S. Liu, K. Wu, C. Jiang, B. Huang, and D. Ma, "Financial time-series forecasting: Towards synergizing performance and interpretability within a hybrid machine learning approach," *arXiv preprint arXiv:2401.00534*, 2023.

[43] D. Brigo, X. Huang, A. Pallavicini, and H. S. D. O. Börde, "Interpretability in deep learning for finance: A case study for the Heston model," *International Journal of Forecasting*, vol. 37, no. 4, pp. 1765–1785, 2021.

[44] M. T. Ribeiro, S. Singh, and C. Guestrin, ""why should i trust you?": Explaining the predictions of any classifier," in *Proceedings of the 22nd ACM SIGKDD International Conference on Knowledge Discovery and Data Mining*, 2016, pp. 1135–1144.

[45] S. M. Lundberg and S. I. Lee, "A unified approach to interpreting model predictions," in *Advances in Neural Information Processing Systems*, vol. 30, 2017, pp. 4765–4774.

[46] B. N. Oreshkin, D. Carpov, N. Chapados, and Y. Bengio, "N-BEATS: Neural basis expansion analysis for interpretable time series forecasting," in *Proceedings of the International Conference on Learning Representations*, 2020.

[47] B. Lim, S. O. Arik, N. Loeff, and T. Pfister, "Temporal fusion transformers for interpretable multi-horizon time series forecasting," *International Journal of Forecasting*, vol. 37, no. 4, pp. 1748–1764, Oct. 2021.

[48] J.-D. Park, K.-M. Kim, and W.-Y. Shin, "CF-KAN: Kolmogorov-arnold network-based collaborative filtering to mitigate catastrophic forgetting in recommender systems," *arXiv preprint arXiv:2409.05878*, 2024.

[49] C. Li, X. Liu, W. Li, C. Wang, H. Liu, Y. Liu, Z. Chen, and Y. Yuan, "U-KAN makes strong backbone for medical image segmentation and generation," *arXiv preprint arXiv:2406.02918*, 2024.

[50] K. Xu, L. Chen, and S. Wang, "Kolmogorov-arnold networks for time series: Bridging predictive power and interpretability," *arXiv preprint arXiv:2406.02496*, 2024.

[51] B. C. Koenig, S. Kim, and S. Deng, "KAN-ODEs: Kolmogorov-arnold network ordinary differential equations for learning dynamical systems and hidden physics," *Computer Methods in Applied Mechanics and Engineering*, vol. 432, p. 117397, 2024.

[52] C. J. Vacca-Rubio, L. Blanco, R. Pereira, and M. Caus, "Kolmogorov-arnold networks (KANs) for time series analysis," *arXiv preprint arXiv:2405.08790*, 2024.

[53] B. Bozorgasl and Y. Chen, "WAV-KAN: A kolmogorov-arnold network with wavelet-based learnable activation functions," *arXiv preprint arXiv:2406.01429*, 2024.

[54] C. Dong, L. Zheng, and W. Chen, "Kolmogorov-arnold networks (KAN) for time series classification and robust analysis," in *Proceedings of the International Conference on Advanced Data Mining and Applications*, 2024, pp. 342–355.

[55] Y. Gao, Z. Hu, W.-A. Chen, M. Liu, and Y. Ruan, "A revolutionary neural network architecture with interpretability and flexibility based on kolmogorov-arnold for solar radiation and temperature forecasting," *Applied Energy*, vol. 378, p. 124844, 2025.

[56] Y. Chen, S. Li, N. Zhao, R. Zheng, and Y. Li, "BiLSTM-KAN: A time series-based traffic flow forecasting model," in *Proceedings of the 2024 13th International Conference on Computing and Pattern Recognition*, 2024, pp. 314–319.

[57] T. Kim, J. Kim, Y. Tae, C. Park, J.-H. Choi, and J. Choo, "Reversible instance normalization for accurate time-series forecasting against distribution shift," in *Proceedings of the International Conference on Learning Representations*, 2022.

[58] Coin Metrics, "Community network data," <https://coinmetrics.io/community-network-data/>, 2025, accessed: 2025.



Yuan Gao received the Ph.D. degree in computer application technology from the Beijing University of Technology in 2016. She completed her post-doctoral research at the State Information Center in 2024. She is currently an Associate Professor with the Department of Electronics and Communication Engineering, Beijing Electronic Science and Technology Institute. Her research interests include blockchain, big data analysis, visualization and computer graphics, and model security.



Zhenguo Dong received the B.S. degree in Computer Science and Technology from the Shandong University of Technology in 2024. He is currently a graduate student with the Beijing Electronic Science and Technology Institute. His research interests include blockchain, multivariate time series forecasting, and model security.



Xuelong Wang received the B.S. degree in micro-electronic science and engineering from the Hefei University of Technology in 2023. He is currently a graduate student with the Beijing Electronic Science and Technology Institute. His research interests include time series data analysis and model security.



Zhiqiang Wang received the Ph.D. degree in Information Security from the School of Communication Engineering, Xidian University in 2015. He is currently an Associate Professor with the Department of Cyberspace Security, Beijing Electronic Science and Technology Institute. His research interests include privacy protection and cyberspace security.



Yong Zhang (Member, IEEE) received the Ph.D. degree in computer science from the Beijing University of Technology in 2010. He is currently a Professor in computer science with the Beijing University of Technology. His research interests include intelligent transportation systems, big data analysis, visualization, and computer graphics.



Shaofan Wang received the B.S. and Ph.D. degrees in mathematics from Dalian University of Technology, Dalian, China in 2003 and 2010, respectively. He is an associate professor from the Faculty of Information Technology, Beijing University of Technology, Beijing, China. His research interest includes pattern recognition and computer vision.